Indian Journal of Pure & Applied Physics
Vol. 56, March 2018, pp. 187-195

Ultrafast adsorption of organic dyes by activated-carbon@Fe_3O_4 nanoscale composites: An effective solution for water purification

Parveen Saini[a,b]*, Rahul Sharma[a,b], R P Pant[c] & R K Kotnala[d]

[a]Conjugated Polymers & Graphene Technology Lab, CSIR-National Physical Laboratory, New Delhi 110 012, India

[b]Academy of Scientific & Innovative Research (AcSIR), New Delhi 110 012, India

[c] EPR Spectroscopy and Magnetic Fluids Section, CSIR-National Physical Laboratory, New Delhi 110 012, India

[d]Spintronics and Magnetic Materials Section, CSIR-National Physical Laboratory, New Delhi 110 012, India

Received 18 June 2017; accepted 6 November 2017

Superparamagnetic (SPM) Fe_3O_4 nanoparticles (NPs) decorated activated charcoal (AC) skeletal (AC@Fe_3O_4) type nanoscale composites (NCs) have been prepared by a scalable and facile approach involving impregnation of AC with stable dispersion of SPM Fe_3O_4 NPs followed by controlled vacuum drying. These NCs exhibit coupled magnetic character and porosity which can be easily optimized by controlling weight ratio of two phases. The electron microscopy images show the presence of clustered Fe_3O_4 particles present all over the surface of porous AC particles and prevalence of meso-pores, which provides the channels for ingress and immobilization of sorbent moieties. The magnetometry and nitrogen adsorption measurements reveal that magnetic character increases whereas porosity decreases with the increase in Fe_3O_4 NP loading. These NCs have been demonstrated for purification of water containing methylene blue (MB) dye as an impurity. The porosity of these composites allow rapid adsorption (<1 min) of MB with good removal efficiency (> 99%) and their magnetic behaviour helps in instantaneous separation of MB adsorbed NC particles by the application of external magnetic field. The sorbent can be reused several times after proper regeneration with retention of more than 95% of the original adsorption capacity.

Keywords: Activated charcoal (AC), Ferrofluid, Fe_3O_4 nanoparticles, Nanocomposites, Superparamagnetism, Methylene blue dye, Water purification, Adsorption

1 Introduction

In past decades, the scarcity of drinking water has become a global crisis as only 2.7% of earth's surface water is potable[1]. The quality and quantity of this precious amount for numerous applications including agricultural, pharmaceutical and industrial uses, are becoming increasingly insufficient due to volatile expansion of global industries and related water pollution hazards[2,3]. It is notable that annual waste water production from both industries and domestic levels is about six times of the existing water in all rivers of the world. The polluted water also poses serious health hazards for organisms and even world health organization (WHO) acknowledged the criticality of the issue by quoting "*in recent past, a number of aquatic species have become extinct and complex biological diseases have generated claiming lives of millions- diarrhea itself killing 2.2 million children annually having age under five*"[4].

In particular, organic dyes that represent important coloring imparting ingredient of leather, paper, textile and rubber industries are also present in significant amount in their waste water streams[5]. Their non-biodegradability and coloring property disturb the biochemical aerobic oxidation based self-purification mechanism of water by preventing penetration of oxygen in water systems. They also interfere with the food cycle and photosynthesis processes of aquatic systems. In humans, their exposure is known to be associated with health hazards varying from irritation, itching, inflammation, nausea and vomiting to more serious ones including carcinogenic and mutagenetic disorders. Therefore, treatment of wastewater containing dyes is of prime importance. Among various dyes, methylene blue (MB) has a special status, due to its large scale consumption in chemical industries (for dying of silk, wool and cotton) and pharmaceutical sector (as indicators, urinary analgesic/anti-infective/anti-spasmodic and as an antidote to potassium cyanide). However, its acute exposure causes increased heart rate, vomiting, shock, cyanosis, jaundice, tissue necrosis or even death[5–7].

Therefore, removal of dyes from wastewater is becoming an increasingly demanding issue and

*Corresponding author (E-mail: pksaini@nplindia.org)

requires viable solutions[6,8–11]. In the past, a number of techniques have been exploited for treatment of dye containing waste water including coagulation, flocculation, membrane filtration and photocatalytic degradation[12,13]. However, these processes suffer from specific disadvantages such as high energy consumption, scalability issues, pollutant selectivity, high cost, low efficiencies and regeneration issues. In this context, adsorption with its simplicity, low cost, environmental friendliness and applicability to diversified pollutants, is considered as most promising commercially viable purification solution. Activated carbon derivatives and other carbon analogues like CNT and graphene or their compositions have been extensively used as adsorbents for variety of water pollutants[6,10,14–20]. Among them, activated charcoal (AC) derivatives[21,22] with high porosity, large specific surface area and low cost, are still the most promising commercially viable options for adsorption based water purification platforms[23–27]. Moreover, adsorption of MB occurs via electrostatic interactions between basic functionalities of dye and acidic functionalities of carbaneous materials and such interactions are not that much strong with less acidic functionalities of CNTs and graphene based composites compared to AC[28]. However, low density and fine particle size of these AC based powdered adsorbents create great difficulty in their removal from purified water especially using filtration or centrifugation operations which represent time consuming processes and considered as non-scalable option[8]. Failure to affect their complete removal may even complicate the situation via recontamination. Interestingly, the micro-meso porous structures of AC materials along with their chemical functionality, provide unique opportunity to integrate them with nanoparticles, thereby expanding their sphere of applicability[23]. It is expected that the AC attached with magnetic nanoparticles can be easily manipulated via external magnetic field, thus become easily handleable. Particularly, the Fe_3O_4 nanoparticles are of great interest due to environmental friendliness, low toxicity, biocompatibility and supermagnetic properties, due to which they have already been exploited for diverse applications ranging from hypothermia treatment, targeted drug delivery, selective burning of tumor etc[29–32]. It is has also been demonstrated that integration of magnetic nanoparticles with various adsorbents enable their magnetic actuation and separation[23]. However, the strong anchoring of magnetic nanoparticles with adsorbent is still difficult due to the presence of non-compatible surface functionalities on nanoparticles and their strong affinity for aqueous acidic media[33]. Attempts to chemically link the magnetic phase with adsorbent provided some success[10] but cannot be considered as commercially viable approach due to process complexity and cost issues.

In present work, Fe_3O_4 nanoparticles decorated AC (AC@ Fe_3O_4) nanoscale composites (FACs) have been synthesized by facile and scalable route involving mixing the organic solvent dispersion of AC with Fe_3O_4 nanoparticles based non-aqueous ferrofluids and subsequent controlled drying. These composites exhibit coupled magnetic character and porous structure, which can be easily optimized by regulation of proportion of two phases. The porosity enables fast adsorption of pollutant molecules whereas magnetic character facilitates rapid magnetic separation of pollutant adsorbed nanoscale composites particles from purified water. The structural, morphological and magnetic properties of these as synthesized FACs have been investigated using powder X-ray diffraction (XRD), vibrating sample magnetometry (VSM), scanning electron microscopy (SEM), transmission electron microscopy (TEM) and high resolution TEM (HRTEM) techniques. Their water purification ability has been demonstrated using water containing MB dye as deliberately added impurity. These composites display fast adsorption of MB and rapid magnetic separation of spent adsorbent. The observed purification performance, simple regeneration, low processing cost, facile synthesis and scalability of the process, make these systems commercially viable water purification alternates, especially for batch phase pretreatment of paper, textile and tannery effluents, before they can be discharged into streams, rivers or other water reservoirs.

2 Experimental Details

2.1 Materials

Activated charcoal (AC), ferrous chloride ($FeCl_2.4H_2O$), ferric chloride ($FeCl_3$), ammonia (25% aqueous solution), MB dye were purchased from Merck and used without further purification. Oleic acid was supplied by Fischer Scientific. Kerosene was purchased locally and double distilled water was used for synthesis or washings.

2.2 Synthesis of oleic acid capped Fe_3O_4 nanoparticles based ferrofluid

Superparamagnetic ferrofluid based on oleic acid capped Fe_3O_4 nanoparticles dispersed in kerosene

was synthesized by wet chemical route involving chemical co-precipitation method[34,35]. In a typical reaction, 1.0 M $FeCl_2.4H_2O$ and 2.0 M $FeCl_3$ aqueous solutions were prepared and mixed under continuous agitation keeping the reaction temperature at 80 °C. After 10 min, 5.0 mL of oleic acid was added, mixture was stirred for 30 min. Subsequently, the oleic acid capped Fe_3O_4 nanoparticles were formed by addition of ammonium hydroxide solution with continuous stirring for 3 h by maintaining the pH and temperature at 12 and 80 °C, respectively, leading to formation of brownish black Fe_3O_4 phase. The formed oleic acid capped particles were settled with the aid of permanent magnet and the supernatant liquid was decanted. The system was washed repeatedly with distilled water and the separated magnetic nanoparticles were dispersed in suitable carrier (kerosene in present case) to 50% solid content. The resultant stable dispersion was dark brown in color and shows formation of characteristic spike of ferrofluids in the presence of permanent magnet (Fig. 1(a)). The formation of Fe_3O_4 phase with crystallite size in the range of 9±1 nm was confirmed by XRD (Fig. 1(b)) as well as HRTEM measurements (Fig. 1(c)). The scratched particles from the dried film of the above ferrofluid display superparamagnetic response (Fig.1(d)).

2.3 Synthesis of Fe_3O_4 decorated AC (AC@Fe_3O_4) nanoscale composites

The Fe_3O_4 decorated AC (AC@Fe_3O_4) NCs were prepared by physical mixing route[36] shown schematically in Fig. 2. In a typical process, about 40 mL of kerosene diluted oleic acid capped Fe_3O_4/kerosene ferrofluid was mixed with known amount of AC powder. The contents were mechanically agitated for 30 min followed by oven drying at 120 °C for 8 h, leading to evaporation of kerosene leaving behind dry NC powder containing Fe_3O_4 decorated AC (AC@Fe_3O_4) particles. Different compositions were prepared by varying the proportion of ferrofluid and AC phases that were designated on the basis of Fe_3O_4 content as FAC1 (pure AC),

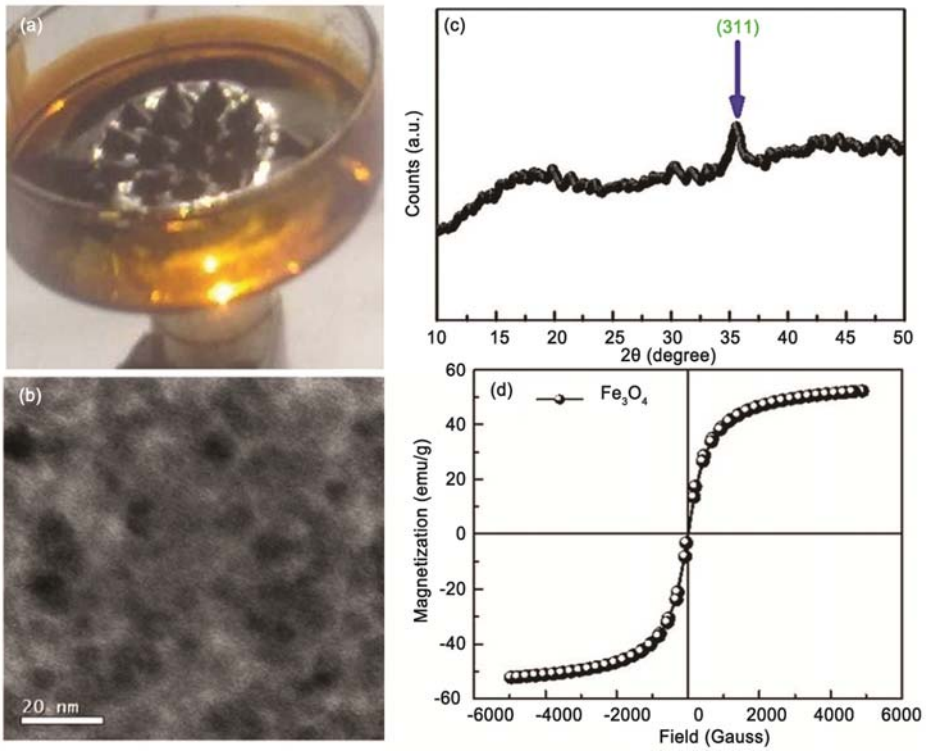

Fig. 1 – (a) Spike formation in ferrofluid dispersion in presence of external magnetic field, (b) HRTEM image of oleic acid capped Fe_3O_4 nanoparticles of the ferrofluid, (c) powder X-ray diffraction pattern of dried film of oleic acid capped Fe_3O_4 nanoparticles based ferrofluid and (d) magnetization response of magnetic particles scratched from dried film of oleic acid capped Fe_3O_4 nanoparticles based ferrofluid displaying superparamagnetic response.

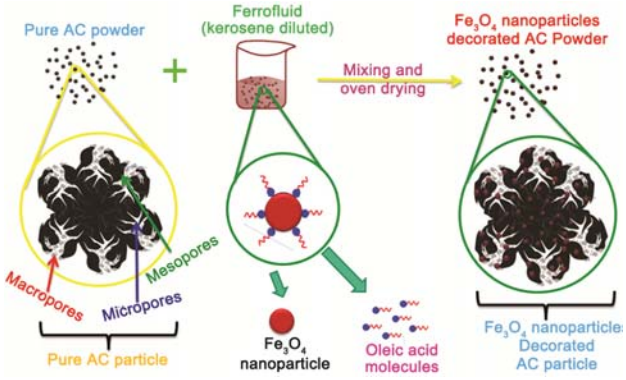

Fig. 2 – Schematic representation of synthesis of Fe_3O_4 nanoparticles decorated AC (AC@Fe_3O_4) NCs.

FAC2 (5 wt% Fe_3O_4), FAC3 (10 wt % Fe_3O_4), FAC4 (22 wt % Fe_3O_4), FAC5 (36 wt % Fe_3O_4) and FAC6 (50 wt % Fe_3O_4).

2.4 Measurements and structural characterization

The characteristic XRD peaks were obtained using Bruker-D8 advanced diffractometer in the 2θ range of (10-70)°. The measurements were taken at scan rate of 0.02°/s, slit width of 0.1 mm and using CuK_α line (λ= 1.540598 Å) as radiation source. Surface morphology was recorded from scanning electron microscope (SEM, model: VP-EVO, MA-10, Carl-Zeiss, UK), attached with energy dispersive X-ray (EDX) analyzer. High resolution transmission electron microscope (HRTEM, model: Tecnai G^2 F30 S-Twin), operating at an accelerating voltage of 300 kV, having a point resolution of 0.2 nm and a lattice resolution of 0.14 nm.), was used for bulk morphological information. The magnetic properties were measured using vibrating sample magnetometer (VSM, model 7304, Lakeshore Cryotronics Inc., USA). The specific surface area (SSA) measurements were performed using BET (Brunauer–Emmett–Teller) surface area analyzer (model: BET 201A, PMI, USA). These composites (FACs) were used for purification of water having 10^{-4} M MB dye as deliberately added impurity.

The adsorption of MB dye molecules on the composites surface was traced using UV- visible spectrophotometer at different time intervals. The dye removal efficiency (%R) and adsorption capacity of FAC adsorbent were calculated from the knowledge of initial and final dye concentration in the aqueous solutions by exploiting the following equations:

$$R = \left(\frac{C_i - C_f}{C_i} \right) \times 100$$

$$q = \frac{\left(C_i - C_f \right)}{m} . V$$

where R is the removal efficiency of adsorbent (expressed in percentage) while C_i and C_f are initial and final dye concentration, respectively. V is total volume of the dye solution and m is mass of adsorbent.

3 Results and Discussion

3.1 Morphological details

Figure 3(a) shows the optical image of AC@Fe_3O_4 NC FAC50 powder which displays magnetic properties and can easily be attracted by permanent magnet (inset of Fig. 3(a)). As the pure AC is non-magnetic in nature, introduction of magnetic functionality is considered as added advantage as it selectively allows the magnetic field assisted separation of NC powder form its physical mixture with non-magnetic material. The SEM micrograph of the NC (Fig. 3(b)) shows the presence of Fe_3O_4 clusters present all over the surface of porous AC particles. The TEM (Fig. 3(c)) image shows the presence of Fe_3O_4 nanoparticles (8-10 nm size marked by green arrow) present over AC particle (yellow dashed line encircled region) whose presence is also confirmed by the position of bright dots in selected area electron diffraction (SAED) pattern (inset of Fig. 3(c)). The high resolution TEM image of AC phase (Fig. 3(d)) shows the presence of mesopores (2-50) nm; some are marked by magenta arrows) which provides the channels for ingress and immobilization of sorbent moieties. The combination of porosity and magnetic character is responsible for fast adsorption and rapid magnetic separation attributes of these NCs.

3.2 XRD analysis

Figure 4 shows the powder XRD patterns of AC and as prepared NCs (FACs). It can be seen that AC displays (Fig. 4(a)) two broad features around 2θ value of 26° and 44°. In comparison, FACs display dominant features of Fe_3O_4 phase and suppression of AC peaks. This confirms that Fe_3O_4 phase forms a uniform coating over AC particles. In particular, the peak at 2θ ~ 35° (yellow arrow) corresponds to 311 planes of single crystalline phase of inverse cubic spinel structure[34,37] of Fe_3O_4. As the Fe_3O_4 content of composites increases (Fig. 4(b-d)), Fe_3O_4 peak progressively dominates the peaks of AC phase, confirming the systematically increasing decoration of Fe_3O_4 nanoparticles over AC

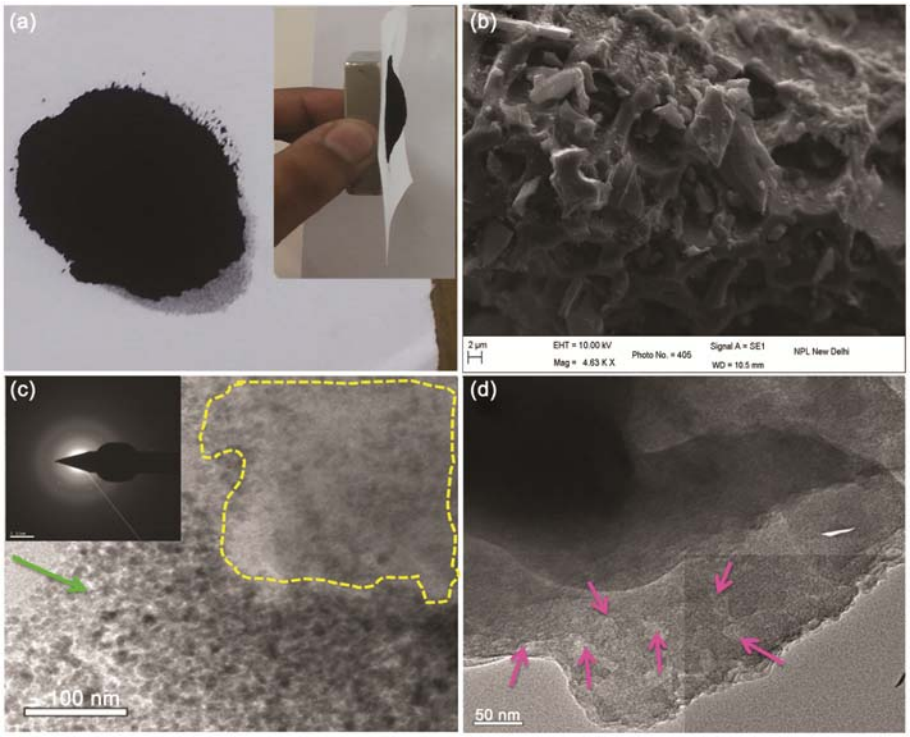

Fig. 3 – (a) Optical image of AC@Fe_3O_4 NC powder and demonstration of its magnetic nature (inset), (b) SEM image of NC powder, (c) TEM image and SAED pattern (inset) of NC and (d) HRTEM image displaying pores present inside AC phase.

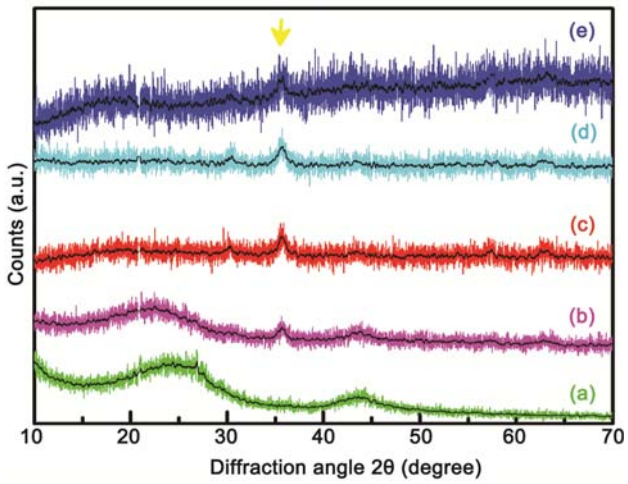

Fig. 4 – XRD patterns of (a) FAC, (b) FAC2, (c) FAC4, (d) FAC6 and (e) oleic acid capped Fe_3O_4 powder scratched from dried ferrofluid film.

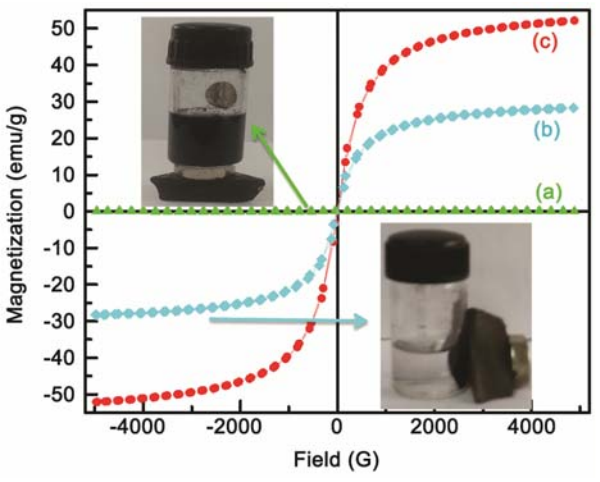

Fig. 5 – VSM curves of (a) AC, (b) FAC6 and (c) oleic acid capped Fe_3O_4 NPs scratched from dried ferrofluid layer.

skeleton. The relatively weak intensity of XRD peaks and their broadness arise due to the very small size of Fe_3O_4 nanoparticles (<10 nm) and presence of oleic acid capping. This also confirms the preservation of nanoparticles features of Fe_3O_4 phase in the formed coating and reflects the formation of nanoscale composites.

3.3 Magnetic properties

Figure 5 shows the VSM curve for the pure AC and its Fe_3O_4 based NCs (FACs). It can be seen (top-left inset) that pure AC particles show non-magnetic character (top left inset) with saturation magnetization (M_s) value of only 0.015 emu/g (Fig. 5(a)). In contrast, Fe_3O_4 nanoparticles display (Fig. 5(c)) typical superparamagnetic (SPM) behaviour (i.e., approximately

zero retentivity and coercivity) with M_s value of 54.3 emu/g. The SPM nature of this sample originates from the fine crystallite size (<10 nm) of Fe_3O_4 particles, which makes it easier for them to be thermally activated to overcome the magnetic anisotropy via randomization even at room temperature[31].

The FAC NCs show moderate magnetization which increases with Fe_3O_4 content. Like Fe_3O_4 nanoparticles, composite also displays negligible hysteresis, which complements the XRD results and again points the preservation of nanoscale features of Fe_3O_4 in the formed coating over AC particles. It is found that FAC6 sample displays good magnetic character with M_s value of 28.3 emu/g (Fig. 5(b)), that enable magnetic field driven separation of MB adsorbed NC particles from the purified water (bottom-right inset), upon the completion of MB dye uptake by the AC phase of the NC. This is considered as significant advantage as magnetic separation is a fast and easy route compared to otherwise time consuming and tedious alternative separation techniques like filtration or centrifugation.

3.4 Adsorption isotherm and specific surface area

Figure 6 shows the BET adsorption isotherms of FAC NCs and variation of their specific surface area (SSA) with Fe_3O_4 nanoparticles content. The shape of the adsorption-desorption curves (Fig. 6(a-c)) resemble a BET type-IV adsorption isotherm[38,39] reflecting the meso-porous nature of samples. It was found that the SSA decreases (Fig. 6(d)) with increasing loading Fe_3O_4 which reflects partial pore clogging by decorated nanoparticles. Therefore, it is apparent that increase in magnetic properties comes at the expense of porosity and surface area. Thus dye adsorption capacity is expected to decrease though magnetic separatibility shows an increase. Accordingly, a composition may be designed on the basis of requirement, i.e., high adsorption capacity or fast magnetic separation.

3.5 Dye removal response and specific adsorption capacity

The water purification ability (including short term adsorption capacity as well as magnetic separation time) of these nanoscale composites has been demonstrated using a known concentration of MB dye as model impurity deliberately added to water as pollutant.

Figure 7 shows the schematic representation of dye sorption process and removal of dye-laden sorbent particles using magnet, leaving behind purified and decolorized water. As the dye solution comes in contact with dispersed adsorbent particles, they

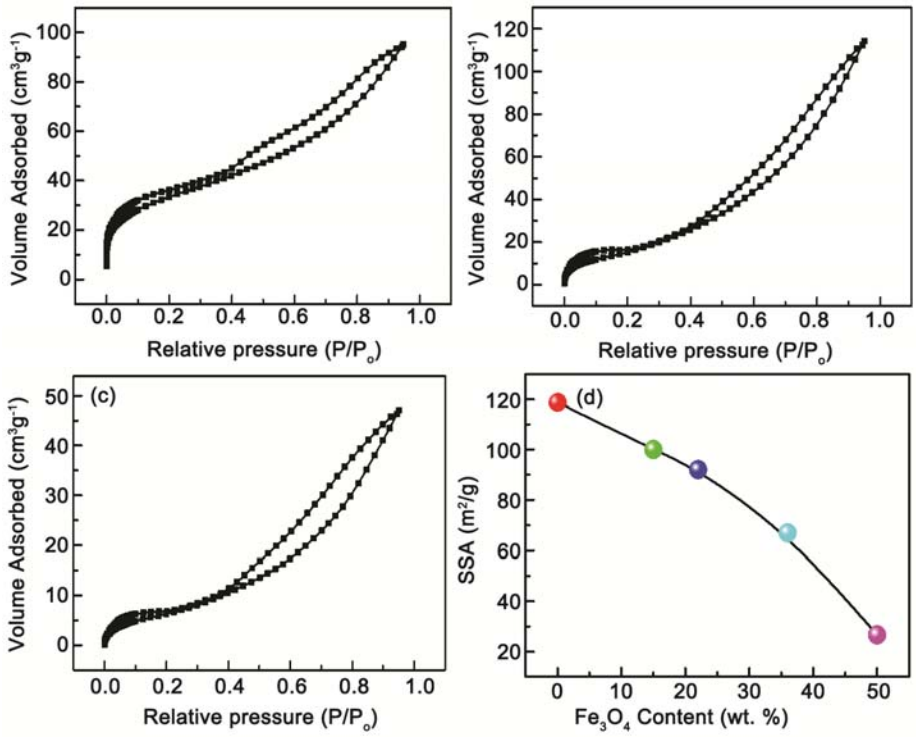

Fig. 6 – Nitrogen adsorption isotherms of FAC nanoscale composites (a) AC, (b) FAC2, (c) FAC6 and (d) variation of SSA of NCs with Fe_3O_4 content.

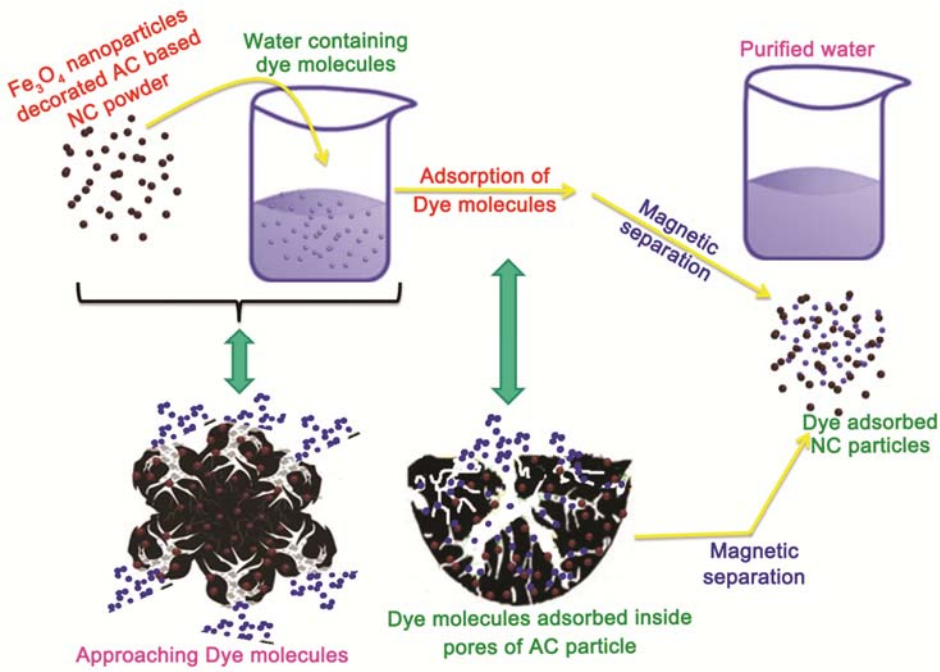

Fig. 7 – Schematic representation of selective adsorption of dye molecules from dye-water mixture using AC@Fe_3O_4 NC powder.

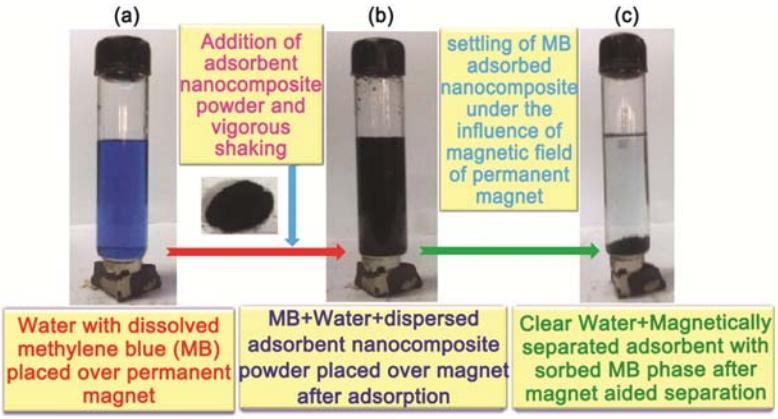

Fig. 8 – Demonstration of water purification using AC@Fe_3O_4 NC containing ~22 wt % of oleic acid capped Fe_3O_4 nanoparticles (FAC4).

rapidly diffuse into the meso- and micro-pores of the sorbent, their flow being channelized via macro-pores and driven by concentration potential difference.

Figure 8 shows digital images of MB solution (Fig. 8(a)), MB solution mixed with FAC4 powder (Fig. 8(b)) and purified water (Fig. 8(c)) with magnetically pulled MB adsorbed FAC4 phase at the bottom of vial. It can be clearly seen that water becomes completely optically transparent (quantitatively <30 ppm dye) after treatment with FAC4 NC and subsequent sorbent particle magnetic settling (video clip of the MB dye removal process can be made available on demand) which reflect high efficiency of purification.

UV-visible spectrophotometery is used to follow the adsorption of MB molecules as a function of time (Fig. 9). The quantification of UV-visible spectra results revealed that MB quickly adsorbs on the FAC4 surface as we can easily see the sharp decrease in the absorbance intensity of MB solution aqueous within 1 min of adorption process (Fig. 9). This FAC4 composite shows short term (less than 1 min time) specific dye adsorption capacity of 9.3 m.mol of MB dye per kilogram of adsorbent powder.

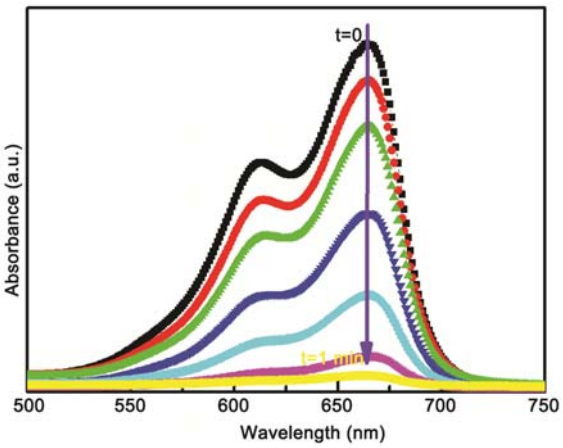

Fig. 9 – UV-visible spectra of MB dye aqueous solutions recorded at different time intervals to trace the adsorption of methylene blue (MB) dye on Fe_3O_4@AC NC containing ~22 wt % of oleic acid capped Fe_3O_4 nanoparticles (FAC4).

Figure 10 shows the magnetic property and MB adsorption capacity of composites as a function of Fe_3O_4 content. It can be seen that incorporation of Fe_3O_4 nanoparticles leads to improvement of magnetic character but at the expense of adsorption capacity, due to increase in clogging of pores by Fe_3O_4 decoaration. Nevertheless, 22 wt% loaded NC (FAC4) shows the good adsorption efficiency and magnetic character to display efficient and fast purification response. In addition to MB which is a cationic dye, the system also works as effective adsorbent for MO a typical anionic dye (Fig. 11). This shows that the adsorption mechanism was not predominantly mediated by ionic integrations. Instead, Van der Waals forces and π-π stacking interactions between adsorbent and dye molecules plays major role.

The good dye removal response and magnetic separation ability of these adsorbents combined with the ease of synthesis and scalability of the process, clearly highlight their potential for effective treatment of various industrial discharge streams rich in organic dyes and also supports their candidature as commercially viable water purification alternates, especially for batch phase pretreatment of paper, textile and tannery effluents, before they can be discharged into streams, rivers or other water reservoirs.

Ability of a sorbent to be amenable towards facile regeneration and subsequent reused several times, without much loss of capacity, is considered as significant advantage in terms of overall economy and energy saving. A batch of such adsorbent may be in use while the other one used in prior purification cycle is undergoing regeneration. Figure 12 shows

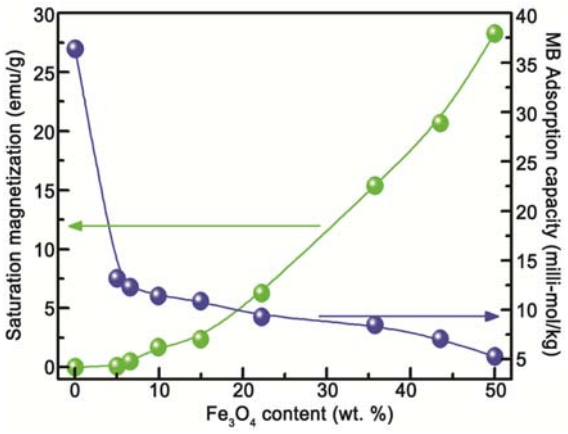

Fig. 10 – Variation of saturation magnetization value and dye adsorption capacity of the AC@Fe_3O_4 NCs as a function of Fe_3O_4 content.

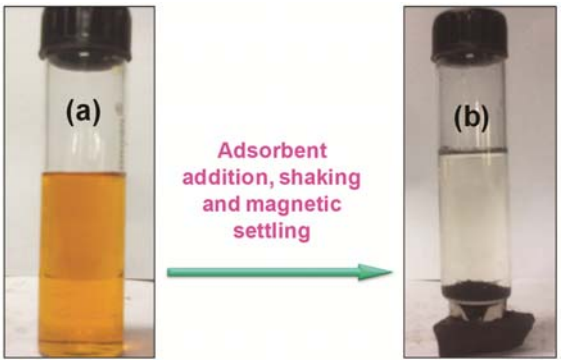

Fig. 11 – Adsorption of methyl orange (MO) dye using Fe_3O_4@AC NC containing ~22 wt % of oleic acid capped Fe_3O_4 nanoparticles (FAC4) followed by magnetic separation of spent adsorbent particles.

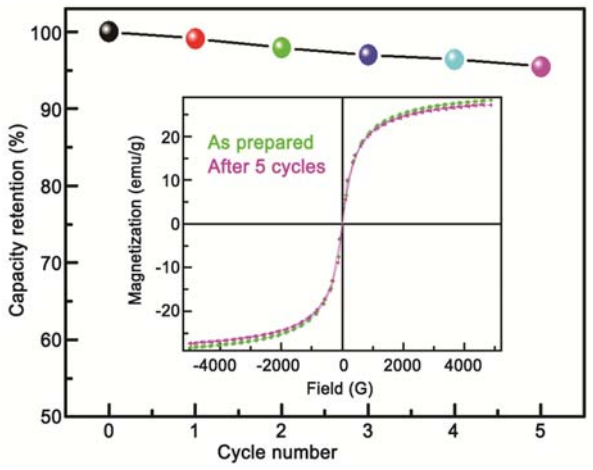

Fig. 12 – Percentage retention of MB dye adsorption capacity of the NC powder as a function of "use-regeneration-reuse" cycles. Inset shows the comparison of VSM plots of the freshly prepared NC powder with the 5 times reused NC powder.

percent retention of specific adsorption capacity of FAC6 NC powder for MB dye as a function of adsorbent use-regeneration-reuse cycle number. After 5-cycles, less than 5% loss in adsorption capacity was observed with no significant loss in magnetic character.

4 Conclusions

SPM Fe_3O_4 nanoparticles decorated activated charcoal NCs (AC@Fe_3O_4) based hybrid adsorbing materials with combination of porosity and magnetic character, have been prepared via a facile and scalable physical mixing process, by systematically varying the proportion of Fe_3O_4. These NCs display good water purification capability by selective adsorption of MB dye present as an impurity. Their porosity enables rapid and efficient adsorption of MB whereas magnetic character allows external magnetic field aided separation of dye laden adsorbent particles. In particular, FAC4 NC display specific adsorption capacity of 9.3 m.mol of MB dye per kilogram of adsorbent, saturation magnetization value of 6.3 emu/g and regenerative reusability with retention of more than 95% of original adsorption capacity after 5 cycles.

Acknowledgement

The authors are grateful to Director, CSIR-National Physical laboratory, New Delhi, for providing necessary research facilities and constant encouragement for this work. Authors are also thankful to Dr N Vijayan for XRD patterns, Mr K N Sood for SEM images, Mr Dinesh Singh for HRTEM and PMI, USA for BET surface area analysis. The work is partially supported by CSIR via CSIR Young Scientist Research Grant (OLP152832).

References

1 Mukherjee R, Sharma R, Saini P & De S, *Env Sci Water Res Technol*, 1 (2015) 893.
2 Elimelech M & Phillip W A, *Science*, (2011) 712.
3 Shannon M A, Bohn P W & Elimelech M, *Nature*, 452 (2008) 310.
4 WWAP (United Nations World Water Assessment Programme). 2014. *The United Nations World Water Development Report 2014: Water and Energy*, Paris, UNESCO.
5 Sulak M T & Yatmaz H C, *Desalination Water Treat*, 37 (2012) 169.
6 Rafatullah M, Sulaiman O, Hashim R & Ahmad A, *J Hazard Mater*, 177 (2010) 70.
7 TOXNET, Toxicology Data Network, Two Democracy Plaza, Suite 440 and Suite 5106707 Democracy Blvd, MSC 5467, Bethesda, MD 20892-5467 https://toxnet.nlm.nih.gov/cgibin/sis/search/a?dbs+hsdb:@term+@DOCNO+1405
8 Barala S K, Arora M & Puri C, *Magnetothermodynamics*, 49 (2013) 277.
9 Wang D W, Li F, Lu G Q & Cheng H M, *Carbon*, 46 (2008) 1593.
10 González Alfaro Y, Aranda P & Fernandes F M, *Adv Mater*, 23 (2011) 5224.
11 Do M H, Phan N H & Nguyen T D, *Chemosphere*, 85 (2011) 1269.
12 Khin M M, Nair A S & Babu V J, *Energy Environ Sci*, 5 (2012) 8075.
13 Jiao T, Guo H & Zhang Q, *Sci Rep*, 5 (2015) 11873.
14 Stavropoulos S & Zabaniotou A, *Materials*, 82 (2005) 79.
15 Sharma P, Hussain N, Borah D J & Das M R, *J Chem Eng Data*, 58 (2013) 3477.
16 Li J, Huang Y & Shao D, *Fundamentals of conjugated polymer blends, copolymers and composites*, Edited by Saini P, (John Wiley & Sons, Inc: Hoboken, NJ, USA), 2015.
17 Kannan N & Sundaram M M, *Dyes Pigments*, 51 (2001) 25.
18 Iqbal M J & Ashiq M N, *J Hazard Mater*, 139 (2007) 57.
19 Fan W, Gao W & Zhang C, *J Mater Chem*, 22 (2012) 25108.
20 El Qada E N, Allen S J & Walker G M, *Chem Eng J*, 135 (2008) 174.
21 Malik P K, *J Hazard Mater*, 113 (2004) 81.
22 Shah I, Adnan R, Wan Ngah W S & Mohamed N, *Plos One*, 10 (2015) 0122603.
23 Safarik I, Horska K, Pospiskova K & Safarikova M, *Int Rev Chem Eng*, 4 (2012) 346.
24 Banat F, Al-Asheh S, Al-Ahmad R & Bni-Khalid F, *Bioresour Technol*, 98 (2007) 3017.
25 Yan C, Wang C & Yao J, *Colloids Surf Physicochem Eng Asp*, 333 (2009) 115.
26 Raposo F, Rubia M A De La & Borja R, *J Hazard Mater*, 165 (2009) 291.
27 Dias J M, Alvim-Ferraz M C M & Almeida M F, *J Environ Manage*, 85 (2007) 833.
28 Ren X, Li J, Tan X & Wang X, *Dalton Trans*, 42 (2013) 5266.
29 Nancy A, Monteiro-Riviere & Lang T C, *Nanotoxicology: Progress toward nanomedicine*, 2nd Edn, (CRC Press Taylor & Francis group: Boca Raton), 2014.
30 Zhao D L, Zhang H L & Zeng X W, *Biomed Mater*, 1 (2006) 198.
31 Qiao R, Yang C & Gao M, *J Mater Chem*, 19 (2009) 6274.
32 Huang S, Li C & Cheng Z, *J Colloid Interface Sci*, 376 (2012) 312.
33 Kong L, Lu X & Bian X, *ACS Appl Mater Interfaces*, 3 (2011) 35.
34 I. Martínez-Mera, Espinosa-Pesqueira M E, Pérez-Hernández R & Arenas-Alatorre , *J Mater Lett*, 61 (2007) 4447.
35 El Ghandoor H, Zidan H M, Khali Mostafa M H & Ismail M I M, *Int J Electrochem Sci*, 7 (2012) 5734.
36 Saini P, Arora A, Kotnala R K, Barala S K, Pant R P & Puri C, W02015044964A1, PCT/IN2014/000636 (CSIR, India) (2015).
37 Zheng Y, Cheng Y, Bao F & Wang Y, *Mater Res Bull*, 41 (2006) 525.
38 Tien C, *Adsorption calculations and modeling*, 2nd Edn, (Butterworth–Heinemann: London), 1994.
39 Khalfaoui M, Knani S, Hachicha M A & Lamine A B, *J Colloid Interface Sci*, 263 (2003) 350.